



A Descriptor for Accurate Predictions of Host Molecules Enabling Ultralong Room-Temperature Phosphorescence in Guest Emitters

Supphachok Chanmungkalakul[†], Chao Wang[†], Rong Miao, Weijie Chi, Davin Tan, Qinglong Qiao, Esther Cai Xia Ang, Choon-Hong Tan, Yu Fang, Zhaochao Xu,^{*} and Xiaogang Liu^{*}

Abstract: Although doping can induce room-temperature phosphorescence (RTP) in heavy-atom free organic systems, it is often challenging to match the host and guest components to achieve efficient intersystem crossing for activating RTP. In this work, we developed a simple descriptor ΔE to predict host molecules for matching the guest RTP emitters, based on the intersystem crossing via higher excited states (ISCHES) mechanism. This descriptor successfully predicted five commercially available host components to pair with naphthalimide (NA) and naphtho[2,3-c]furan-1,3-dione (2,3-NA) emitters with a high accuracy of 83%. The yielded pairs exhibited bright yellow and green RTP with the quantum efficiency up to 0.4 and lifetime up to 1.67 s, respectively. Using these RTP pairs, we successfully achieved multi-layer message encryption. The ΔE descriptor could provide an efficient way for developing doping-induced RTP materials.

Introduction

Room-temperature phosphorescence (RTP) in heavy-atom free organic materials has been attracting significant research interest,^[1,2] for both fundamental photophysics and their promising potentials in numerous applications, i.e.,

electronic displays,^[3] security ink,^[4–9] and bio-imaging.^[10,11] Indeed, the last decade has witnessed the rapid development of nascent RTP materials emitting bright and/or persistent luminescence at ambient conditions.^[1] Along with this exciting progress, several molecular design strategies have been proposed to guide the rational development of heavy-atom free RTP materials,^[12] such as the incorporation of a lone-pair electron moiety (i.e., carbonyl group),^[13] narrowing singlet–triplet gaps in twisted donor–acceptor molecules,^[14] host–guest complexation,^[15] polymerization,^[16,17] packing efficiency tuning,^[18] H-bond immobilization,^[19] and supramolecular interaction.^[20]

In particular, doping host materials (majority) with guest emitters (minority) through simple mixing represents one favorable method to generate RTP with ultralong lifetime (or afterglow), for its ease of processing, abundant availability of raw materials, tunable colors, and low cost (Scheme 1a).^[21] Doping has already been frequently employed in creating inorganic phosphorescent materials for more than two decades, such as the doping of Dy³⁺ into the SrAl₂O₄:Eu²⁺ phosphor to yield afterglow, which peaked at 520 nm.^[22] Recently, in a landmark study, Liu and co-workers showed that the afterglow of an organic emitter, carbazole, was induced by trace amounts of carbazole isomer impurities.^[23] In another milestone work, Tang et al. demonstrated that doping a naphthalene emitter in several solid small-molecule matrices produced strong and persistent RTP.^[21] Ma and co-workers also reported a series of host/guest molecular combinations, which provided persistent RTP after the addition of a trace amount of impurities; they further confirmed that the phosphorescence emitters are the impurities (guest molecules).^[24] Despite these excellent studies, the detailed RTP working mechanism for multiple-molecular systems, especially the intersystem crossing (ISC) process from singlets to triplets, remains controversial. As a result, laborious trial-and-error is often unavoidable in the development of organic afterglow materials as the guideline of inducing efficient ISC is still lacking.

Along with these trials-and-errors, many research efforts have been focused on inducing ISC from S₁ to T_n (instead of S_n to T_n transitions) in organic afterglow materials. This approach is valid for most single-molecular systems, because rapid internal conversion processes will quickly bring excited molecules from S_n to S₁ before ISC takes place. To this end, it is generally agreed that a small singlet–triplet gap and

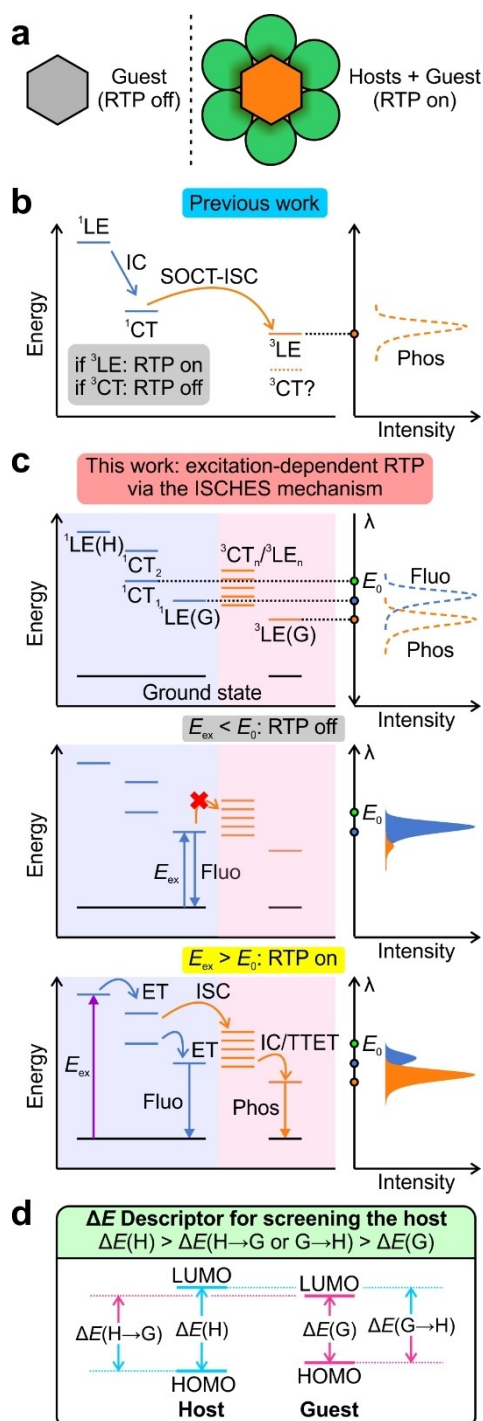
[*] S. Chanmungkalakul,[†] Dr. C. Wang,[†] Dr. W. Chi, Dr. D. Tan, Prof. Dr. X. Liu
 Fluorescence Research Group, Singapore University of Technology and Design, 8 Somapah Road, Singapore 487372 (Singapore)
 E-mail: xiaogang_liu@sutd.edu.sg

Dr. C. Wang,[†] Dr. Q. Qiao, Prof. Dr. Z. Xu
 CAS Key Laboratory of Separation Science for Analytical Chemistry, Dalian Institute of Chemical Physics, Chinese Academy of Sciences, 457 Zhongshan Road, Dalian 116023 (China)
 E-mail: zcxu@dicp.ac.cn

Prof. Dr. R. Miao, Prof. Dr. Y. Fang
 Key Laboratory of Applied Surface and Colloids Chemistry, Ministry of Education, School of Chemistry and Chemical Engineering, Shaanxi Normal University, Xi'an 710062 (China)

E. C. X. Ang, Prof. Dr. C.-H. Tan
 School of Physical and Mathematical Sciences, Nanyang Technological University, 21 Nanyang Link, Singapore 637371 (Singapore)

[†] These authors contributed equally to this work.



Scheme 1. a) Schematic illustration of doping-induced RTP in purely organic molecules. b) The spin-orbit charge-transfer ISC (SOCT-ISC) mechanism to induce RTP. c) Proposed mechanism of intersystem crossing via higher excited states (ISCHES). d) Schematic illustration of the ΔE descriptor for screening RTP materials. ET: energy transfer; IC: internal conversion; TTET: triplet–triplet energy transfer; Fluo: fluorescence; Phos: phosphorescence. H and G represent host and guest, respectively.

large spin-orbital coupling (SOC) matrix elements can greatly enhance the ISC process.^[25] Moreover, when S_1 and T_1 displayed a charge-transfer (CT) and locally excited (LE)

characteristics, respectively, ISC can be significantly enhanced via the spin-orbit charge-transfer ISC (SOCT-ISC) mechanism (Scheme 1b).^[6,26–31] However, in the multiple-molecular system (such as doping of host with guest molecules), multiple S_1 of different components can co-exist.^[32] In addition to the most stable S_1 , other less stable “ S_1 ” or higher excited singlet states (S_n) of the system may also play important roles in promoting ISC and enabling RTP. This readily occurs when the ISC rate from S_n to T_n is comparable with the intermolecular energy transfer rate from S_n to S_1 . Yet, the study of S_n to T_n transitions in dual/multiple-molecular systems has been relatively neglected or overlooked.

Herein, we demonstrated excitation-dependent RTP generations and showed that $S_n \rightarrow T_n$ transitions played a crucial role in enabling afterglows in the host/guest systems (Scheme 1c). As a result, when the excitation energy (E_{ex}) is smaller than the threshold E_0 , RTP is disabled; when $E_{ex} > E_0$, RTP is enabled. We rationalized this excitation dependence by establishing an intersystem crossing via higher excited states (ISCHES) mechanism, buttressed by detailed quantum-chemical calculations and spectroscopic data. We further proposed and validated a simple ISCHES descriptor, ΔE , to accurately and rapidly screen host materials to enable bright and persistent RTP in guest emitters (Scheme 1d). The ΔE descriptor is expected to greatly facilitate the quantitative development of RTP materials.

Results and Discussion

Inspired by the excellent experimental results of previous studies,^[21] we first investigated the RTP mechanism in a known host/guest system, H1/NA (Figure 1a–c). We noted that the guest molecule (NA) alone did not produce any notable afterglow at room temperature, but the mixture of H1/NA ($w:w=99:1$) emits bright RTP (Figures S1), with a phosphorescence lifetime of 678 ms and a good quantum yield ($\phi_{F+P}=0.243$; Tables S1 and S2). Of noteworthy, H1/NA exhibited an unusual excitation-dependent photoluminescence spectrum. As the short excitation wavelengths (≤ 310 nm) matched the UV/Vis absorption spectra of the host molecules, strong phosphorescence, in addition to bright fluorescence from the guest emitters, was observed. As the excitation light was shifted to a longer wavelength region which can be directly absorbed by the guest molecules (≥ 310 nm), only intense fluorescence from the guest emitters was observed, with almost negligible phosphorescence.

To further demonstrate this excitation dependence, we calculated the ratio (P/F) between the phosphorescence and fluorescence intensities as a function of the excitation wavelength (Figure 1c). This ratio eliminates the impact of the variation in the UV/Vis absorbance over these excitation wavelengths. In the host/guest pair H1/NA, as the excitation wavelength becomes longer than ≈ 320 nm (around the cutoff UV/Vis absorption wavelength of H1), a significant reduction in P/F was observed (Figure 1c, Figures S2–S5). This excitation dependence demonstrated that higher excited states S_n (or short-wavelength absorption) play an

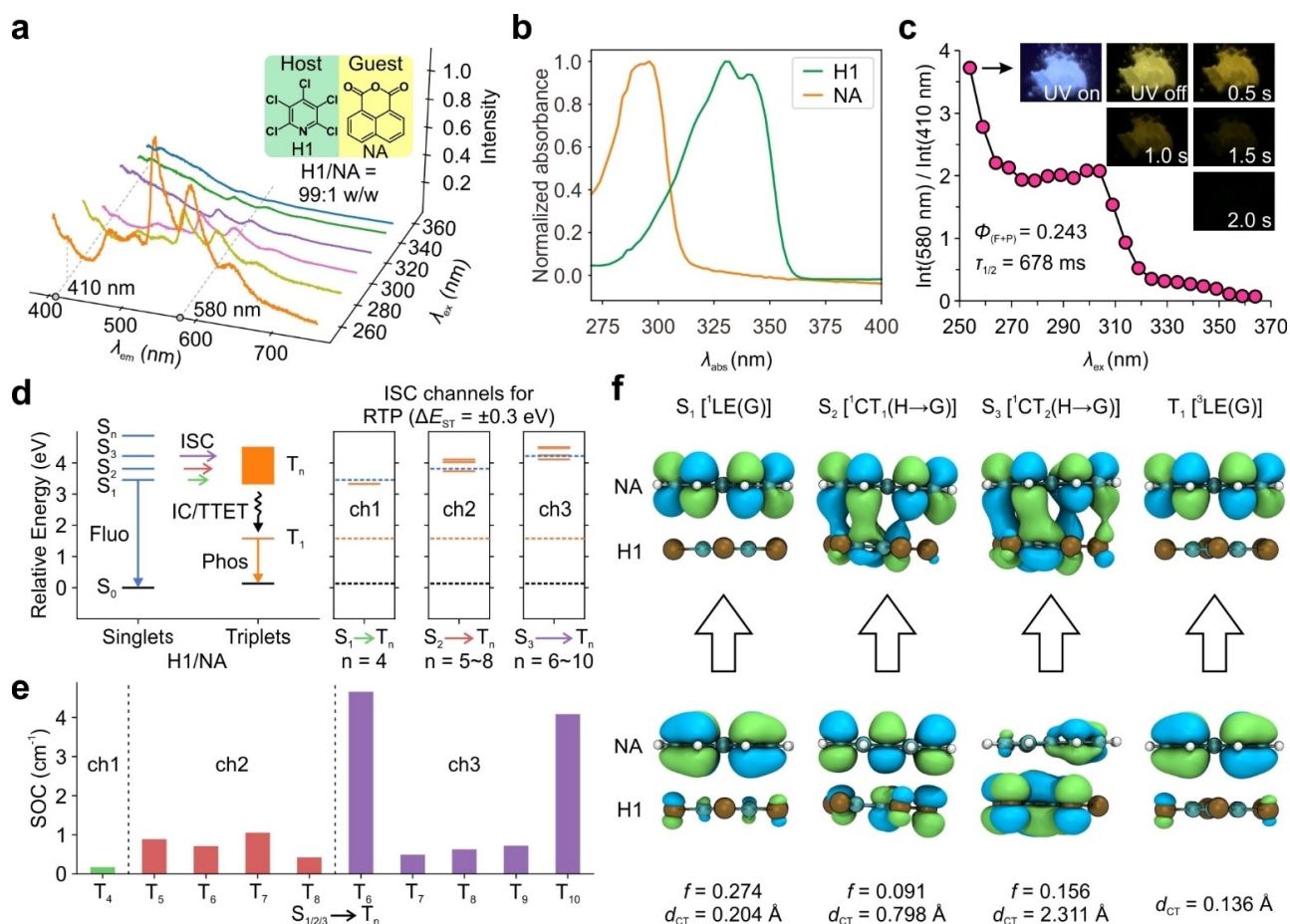


Figure 1. a) Excitation–emission matrix (EEM) of H1/NA. b) Normalized UV/Vis absorption spectra of H1 and NA in chloroform. c) Ratio plot between phosphorescence intensity (580 nm) and fluorescence intensity (410 nm) derived from EEM plot at various excitation wavelengths with emission pictures of the compound before and after turning off 254 nm excitation light. d) The relative energy of H1/HA and the ISC channels for RTP calculated at the CAM-B3LYP/Def2-SVP level in chloroform. e) The corresponding SOC matrix element of various ISC channels for RTP. f) The corresponding hole and electron NTOs of S_1 , S_2 , S_3 , and T_1 . The S_n energy level was estimated from the H1 monomer, while the energy levels of S_1 , S_2 , S_3 , and T_1 are derived from the H1/NA dimer. All excited-state calculations were conducted at the CAM-B3LYP/Def2-SVP level in chloroform.

indispensable role in promoting ISC and activating RTP in the host/guest system.

During these experiments, we have ensured that the host and guest molecules are of high purities, and the results are not compromised by other impurities (Table S3 and Figures S6–S17).

Subsequently, detailed quantum chemical calculations were conducted to rationalize the excitation-dependent RTP generation in H1/NA (Figure 1d–f). To this end, we modeled an H1 and NA dimer as a simple model to gain insights into the host/guest interactions. In this host/guest dimer system, our calculations revealed three types of low-lying singlet excited states: 1) the ${}^1\text{LE}(\text{H})$ state localized on the host, corresponding to S_1 of the host molecule or S_n of the host/guest dimer system, 2) the ${}^1\text{LE}(\text{G})$ localized on the guest molecules, corresponding to the S_1 of the guest molecule and S_1 of the host/guest dimer system, and 3) two low-lying charge-transfer (CT) states involving the host/guest complex, i.e., the ${}^1\text{CT}_1(\text{H}\rightarrow\text{G})$ and ${}^1\text{CT}_2(\text{H}\rightarrow\text{G})$ corresponding to S_2 and S_3 of the host/guest dimer system, respectively (Figure 1d,f).

It is worth mentioning that the conversions between various singlet states in different components take place by energy transfer rather than internal conversion. Internal conversion in the traditional Jablonski diagram governs $S_n\rightarrow S_1$ transitions within a single molecular system. However, the singlet states in the host/guest mixture involve three different molecular systems: the host, the host/guest complex, and the guest, as an extended version of the Jablonski diagram. The energy transfer rate between these molecular systems is much slower than the internal conversion within a single molecule, endowing sufficient $S_1\text{--}S_n$ lifetime in this multiple-molecule system for other photophysical processes to occur, such as ISC via higher excited singlet states.

Next, we optimized the geometries of the host/guest dimer system in the excited states S_1 , S_2 , and S_3 , respectively, and calculated the corresponding spin-orbit coupling (SOC) matrix elements between these singlet states and their respective close-lying triplet states (± 0.3 eV). A small energy gap between these singlet and triplet states (ΔE_{ST}) and a large SOC value are two important prerequisites to ensure high ISC rates.^[25] Notably, SOC from S_1 to its close-

lying triplet states (0.17 cm^{-1}) was found to be very small, while SOC from S_2 (from 0.43 to 1.06 cm^{-1}) and S_3 (from 0.49 to 4.66 cm^{-1}) to close-lying triplet states were significantly larger, by up to 27.4 times (Figure 1d,e).

To understand these different SOC values, we further analyzed the electronic structures of these excited states. To this end, the natural transition orbitals (NTOs) can provide a more compact orbital representation than the original molecular orbitals (MOs), especially when multiple MO pairs are involved in the excitation of a high-lying excited state.^[33] In addition, charge transfer distance (d_{CT}) measures the distance between the positive and negative charge centroids involved in the excitations.^[34] Thus, it can be used to quantify the degree of charge transfer to distinguish the CT and LE states. Based on both NTO and d_{CT} analysis, the electron and hole distributions revealed that that S_1 of the host/guest dimer system is an LE state centered within the guest molecule, while both S_2 and S_3 represent a CT state spanning across the entire host/guest complex. Concurrently, many triplet states are mostly LE states centered either in the guest or host molecule. According to the El-Sayed rule, the ISC rate can be enhanced when there is a significant change between the nature of the singlet and triplet excited states.^[35–37] Accordingly, our computational results suggest that higher excited CT states (S_2 and S_3) are crucial pathways for efficient ISC in H1/NA, which is in excellent agreement with experimental observations.

Lastly, our calculations revealed that the T_1 of the host/guest dimer system is an LE state located in the guest molecule (Figure 1f). This result suggests that after ISC, internal conversions and/or triplet-triplet energy transfer eventually conveys the absorbed photon energy to the guest emitter, enabling bright and persistent afterglow in H1/NA.

All in all, our computational results can be used to rationalize the excitation dependence of RTP generations in H1/NA (Scheme 1c). Upon short-wavelength photoexcitation, the energy of higher excited states S_n (mostly absorbed by host molecules) could transfer either to the charge-separated states, S_2 [$^1CT_1(H\rightarrow G)$] and S_3 [$^1CT_2(H\rightarrow G)$], which are associated with the host/guest complex, or to the S_1 [$^1LE(G)$] state of the guest molecule NA. Subsequently, energy in S_2 [$^1CT_1(H\rightarrow G)$] and S_3 [$^1CT_2(H\rightarrow G)$] could either transfer to S_1 [$^1LE(G)$], resulting in intense fluorescence, or transfer to the high-lying triplet states of host/guest molecules, T_n , via ISC. This triplet state energy will eventually cascade to T_1 [$^3LE(G)$], resulting in RTP. During this process, the relatively slow singlet energy transfer processes, and the enhanced ISC are two key factors in activating bright RTP. In contrast, long-wavelength photoexcitation is directly absorbed by S_1 [$^1LE(G)$] and cannot induce efficient ISC via these higher excited states. In this case, almost all of the energy will be released from S_1 of NA as fluorescence and nonradiative decays. Accordingly, long-wavelength photoexcitation can only turn on bright fluorescence and very weak RTP. We coin this excitation-dependent RTP generation mechanism, as exemplified in the bimolecular H1/NA system, as intersystem crossing via higher excited states (ISCHEs).

Inspired by the ISCHES mechanism, we next aimed to establish a simple descriptor to allow for accurate prediction of host materials that can enable persistent RTP of guest emitters. To this end, three important factors must be considered: 1) efficient intersystem crossing from singlet to triplet excited state;^[36,38] 2) slow radiative rate from the triplet states (k_{tr}) to maintain long phosphorescence lifetime;^[2] 3) negligible nonradiative decays from the triplet state (k_{nr}) to ensure the good quantum yield of phosphorescence.^[39] The first requirement could be effectively addressed via the newly established ISCHES mechanism. The second requirement can be fulfilled by carefully choosing a good phosphorescence emitter whose first triplet excited state (T_1) exhibits $\pi-\pi^*$ transition characteristic, as radiative transitions from $T_1(\pi-\pi^*)$ to the ground state (S_0) is typically much slower than that from $T_1(n-\pi^*)$.^[13] Many reported emitters are good potential candidates, such as naphthalimide,^[40] carbazole,^[10,23] triphenylamine derivatives,^[41] and 1,8-naphthalic anhydride.^[21] The last requirement could be achieved in tightly packed solid-state systems, where oxygen penetration, exposure, and associated quenching are minimized and nonradiative vibrations are largely inhibited.

To simplify the already complicated excited-state calculations, we assumed that the electronic gaps, derived from simple ground-state calculations of the host and guest monomers, may serve as a good descriptor for the ISCHES mechanism (Figure 2a). For example, the electronic gaps between the highest occupied molecular orbital (HOMO) and the lowest unoccupied molecular orbital (LUMO) of the host [$\Delta E(H)$], and between the HOMO and LUMO of the guest [$\Delta E(G)$], can be approximated as optical gaps of the LE states of the host [$^1LE(H)$] and guest [$^1LE(G)$] molecules, respectively, as these transitions typically take place in either bare host or guest molecules. The electronic gaps between the host's HOMO and the guest's LUMO [$\Delta E(H\rightarrow G)$] and between guest's HOMO and host's LUMO [$\Delta E(G\rightarrow H)$] correspond to the charge-transfer (CT) states [$^1CT(H\rightarrow G$ or $G\rightarrow H)$], as these transitions involve charge transfer between the host and guest molecules. Following the ISCHES mechanism, where the $^1LE(H) > ^1CT(H\rightarrow G$ or $G\rightarrow H) > ^1LE(G)$, we reasoned that ΔE might serve as a useful descriptor to screen the host matrices for guest RTP emitters, as long as the following condition is fulfilled: $\Delta E(H) > \Delta E(H\rightarrow G$ or $G\rightarrow H) > \Delta E(G)$. It is also noteworthy that similar ground state MO descriptors have been reported to provide reliable insight in designing and screening luminescent functional materials and probes.^[42,43]

To experimentally verify our descriptor-based screening method, 16 different host materials (99% weight) were selected and physically mixed with the known afterglow emitter NA (1% weight; Figure 2b; Tables S1 and S2). These 16 host materials were chosen based on the ease of their commercial availability, as common laboratory reagents. Host molecules that contain minimal steric hindrance were chosen to ensure close packing with the guest molecule, thereby, enhancing the probability of generating an effective charge transfer state between them. These 16

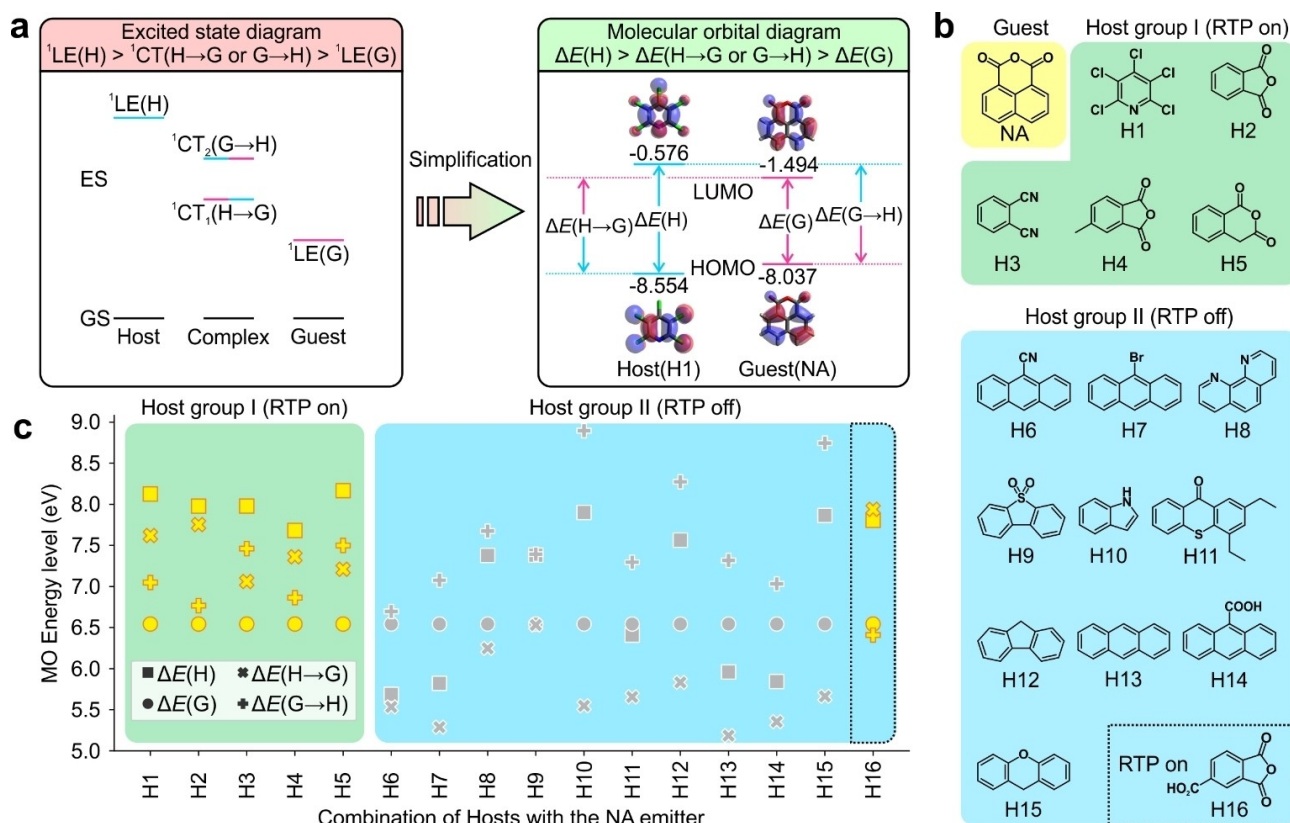


Figure 2. a) Illustration of excited state energy diagram of the host, guest, and complex in Group I represented by ${}^1\text{LE}(\text{H}) > {}^1\text{CT}(\text{H}\rightarrow\text{G} \text{ or } \text{G}\rightarrow\text{H}) > {}^1\text{LE}(\text{G})$ (left) and an example of ΔE calculation of H1/NA satisfying the condition of $\Delta E(\text{H}) > \Delta E(\text{H}\rightarrow\text{G} \text{ or } \text{G}\rightarrow\text{H}) > \Delta E(\text{G})$ (right). b) Chemical structures of the NA emitter and host molecules in Group I and Group II. c) Calculated electronic gaps of host/NA pairs at the CAM-B3LYP/Def2-SVP level. All these calculations were conducted in chloroform (to mimic the low polarity environment of the solid-state materials) using the SMD model. LE: locally excited state; CT: charge-transfer state; H: host; G: guest (the RTP emitter).

host/guest combinations form a training dataset for our search for a quantum chemical descriptor.

Initial molecular modeling calculations involved geometry optimizations of all host and guest monomers in the ground state in chloroform (to mimic the low polarity of the solid-state matrices) using the CAM-B3LYP/def2-SVP level of theory. It was observed that these HOMOs and LUMOs delocalized across the entire host or guest molecules (Figures S18–S35). Next, we divided these host molecules into two groups. Group I meets the ISCHES requirement with $\Delta E(\text{H}) > \Delta E(\text{H}\rightarrow\text{G} \text{ or } \text{G}\rightarrow\text{H}) > \Delta E(\text{G})$; Group II does not satisfy the ISCHES requirement, with a low lying $\Delta E(\text{H}\rightarrow\text{G})$ or $\Delta E(\text{G}\rightarrow\text{H})$ gap (Figure 2c).

To this end, we also applied other computational methods to validate the consistency of our results. We found that M062X, CAM-B3LYP, and ω B97X-D functionals led to the same grouping of these host materials, based on the energy levels of the frontier molecular orbitals (Figures S36 and S37).

Subsequent experimental observations revealed an excellent correlation between our quantum chemical descriptors ΔE and host/guest combos with afterglows. In Group I, all five host/guest molecule pairs emit bright and persistent RTP; moreover, these five pairs exhibited excitation-dependent RTP generations (Figure 2c; Figures S38–S53).

The phosphorescence spectra were also consistent in these samples, attributed to the LE state of the guest emitter. These results, buttressed by additional excited-state calculations (Figures S54 and S55), corroborate the proposed ISCHES mechanism. These results also strongly suggest that ΔE would serve as a useful descriptor to screen host molecules for the discovery of afterglow materials.

In contrast, 10 out of 11 host/guest pair molecules in Group II did not produce afterglows (Figure 2c). Additional computational investigations were subsequently performed to explain this. As shown by the low-lying $\Delta E(\text{H}\rightarrow\text{G})$ or $\Delta E(\text{G}\rightarrow\text{H})$ in the host/guest H10/NA pair, the most stable T_1 state mapped to the ${}^3\text{CT}$ of the host/guest complex, instead of the guest molecule ${}^3\text{LE}$ (Figure S56; Scheme 1b). As a result, H10/NA did not yield bright RTP as the ${}^3\text{CT}$ is usually non-emissive. Similarly, although the host molecule contains n- π bonds (H6), heavy atoms (H7), carbonyl groups (H14), the host-guest pairs would not provide RTP if the HOMO–LUMO energy level did not match with the ISCHES requirements.

In addition, some Group II pairs can produce RTPs if their ${}^3\text{LE}$ is located below or close to ${}^3\text{CT}$. Although ${}^3\text{CT}$ is slightly lower than ${}^3\text{LE}$ in H16/NA, the small energy difference (0.03 eV) may result in the mixing of ${}^3\text{LE}$ and ${}^3\text{CT}$, thus enabling RTP (Figure S56).

By considering these factors, we decided to employ ΔE as our descriptor and $\Delta E(\text{H}) > \Delta E(\text{H} \rightarrow \text{G} \text{ or } \text{G} \rightarrow \text{H}) > \Delta E(\text{G})$ as our ISCHES conditions to screen various host molecules. This would lead to only Group I combos, and inevitably miss some possible bright Group II combos. However, this conservative choice enhances the success rate of host material screening. Moreover, this ΔE descriptor only requires simple ground-state calculations of monomers, and can be easily scaled up for large-scale material discovery and screening. Finally, it is worth mentioning again that we limit our host molecules to quasi-planar compounds to ensure close host-guest distances and strong electronic interactions between them to generate stable CT states.

Encouraged by our results see above, we predicted two new host materials (H17 and H18) for the guest emitter NA (Figures 3a, b, S34–S37). These three host molecules are of low cost and commercially available compounds and possess planar conformations to ensure close host/guest molecular packing. According to our ground-state calculations, the HOMO and LUMO energy levels of the guest molecule are sandwiched between those of the two host molecules, thus meeting the requirements outlined earlier: $\Delta E(\text{H}) > \Delta E(\text{H} \rightarrow \text{G} \text{ or } \text{G} \rightarrow \text{H}) > \Delta E(\text{G})$.

Subsequent experiments further confirmed the accuracy of our predictions. The H17/NA and H18/NA pairs emitted bright and persistent RTP (with a lifetime of 523 ms and 620 ms, respectively; and photoluminescence quantum yields

($\phi_{\text{F+P}}$) of 0.08 and 0.06, respectively; Tables S1 and S2). Both pairs also exhibited excitation dependence in RTP generations, obeying the ISCHES mechanism.

We also extended our host screening method to another phosphorescence emitter 2,3-naphthalenedicarboxylic anhydride (2,3-NA) (Figure 3c). Based on the candidate pool of 18 host materials (as used in the previous experiments), our calculation predicted that four host molecules could activate afterglow in 2,3-NA (Figures S57–S78). Subsequent experiments showed that unpaired solid 2,3-NA did not produce any observable phosphorescence. However, 3 out of 4 host/guest pairings (including H1/2,3-NA, H5/2,3-NA, and H18/2,3-NA) exhibited bright afterglow, with a lifetime of 1107, 445, and 1669 ms, respectively (Tables S4 and S5; Figures S79–S86). Likewise, excitation-dependent RTP emissions were observed in these systems; only short-wavelength light (absorbed by the host molecules) enabled afterglow. Notably, different from NA's yellow phosphorescence (with a peak at 587 nm), 2,3-NA emits green phosphorescence peaked at 510 nm and the green phosphorescence was observed in all these three combos (Figure 3d). These experimental results further demonstrated the effectiveness and accuracy of our descriptor-based host screening method to activate afterglow in guest emitters.

The only outlier (H9/2,3-NA) could be caused by other factors such as solid-state packing modes and contributions from exciton binding (the difference between electronic and

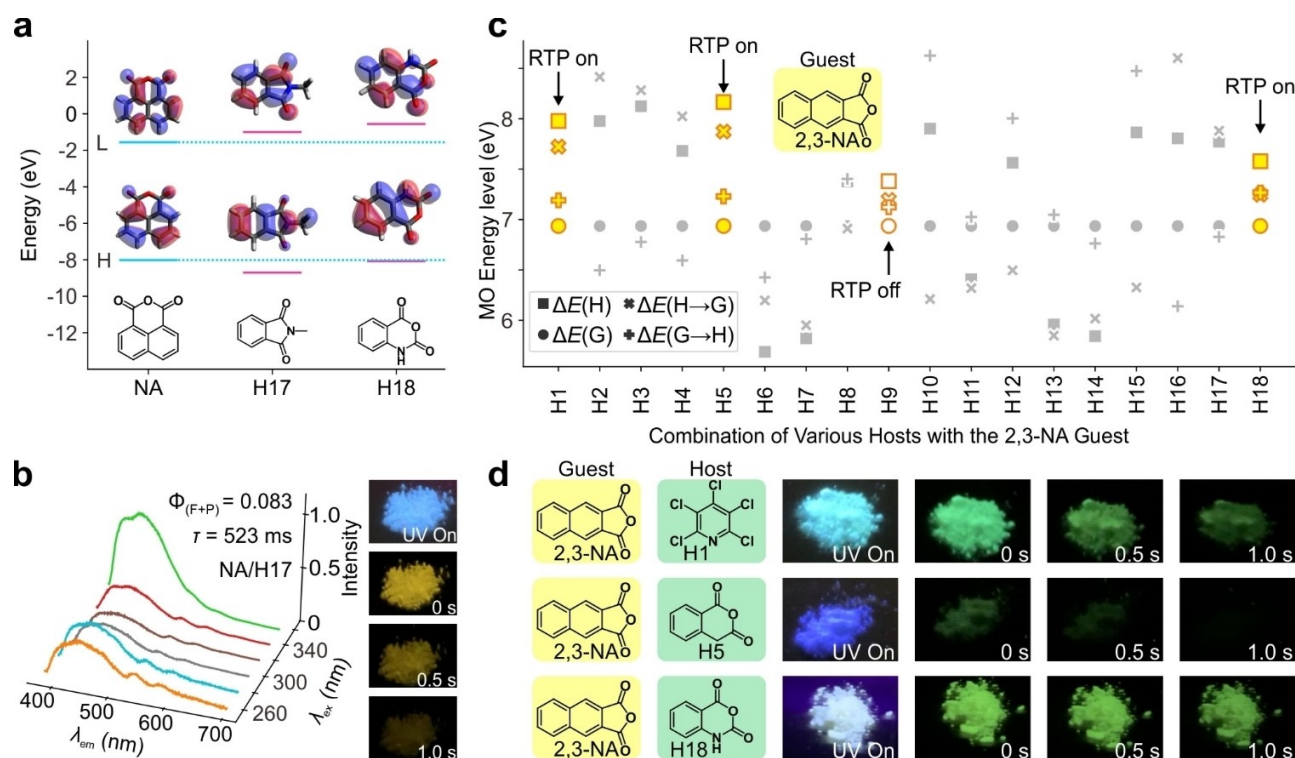


Figure 3. a) Calculated molecular orbital energy diagram of NA, H17, and H18. b) Excitation-emission matrix of H17/NA with emission pictures of the compound before and after turning off 254 nm excitation light. c) Calculated electronic gaps of host/2,3-NA pairs obtained from the ΔE screening with emission pictures of the compound before and after turning off 254 nm excitation light. The electronic gaps are derived from calculations conducted at the CAM-B3LYP/Def2-SVP level of theory in chloroform (to mimic the low polarity environment of the solid-state materials) using the SMD model.

optical gaps), which our descriptor does not account for. These factors could also play critical roles in some RTP molecular systems.

Lastly, we demonstrated an application as a possible multi-layer security encryption (Figure 4a), based on two host/guest combinations, H18/NA (w:w=99:1), and H18/2,3-NA (w:w=99:1). Host H18 was chosen as it responded well to both guests (NA and 2,3-NA). The two pairs emit bright yellow (lifetime = 620 ms) and green afterglows (lifetime = 1669 ms), respectively.

Benefiting from the different lifetime intervals, a simple double-layer encryption system could be set up (Figure 4b). First, a filter paper was soaked in an acetone solution of H18 and subsequently dried at room temperature. Ink tubes of gel pens were cleaned and re-filled with a saturated solution of NA or 2,3-NA in alcohol (1:1 MeOH/1-propanol). The pen was then used to inscribe a two-layer coded message on the filter paper. As shown in Figure 4b, upon shining and switching off a UV light source, the inscribed message “SUTD FRG” was observed. After 1 s, the yellow “SUTD” disappeared, while the green “FRG” remained. Such use of different RTP emitters with different emission wavelengths and lifetimes via simple pairing with

the same host material can be used for multi-layered message encryption technology.

Conclusion

In conclusion, we have proposed an ISCHES mechanism to rationalize the excitation-dependent RTP generations in many host/guest systems. This includes establishing a simple yet effective descriptor ΔE to screen various host materials to discover and enable bright and persistent RTP of guest emitters at ambient conditions. With the aid of ΔE , we successfully predicted five host materials for two emitters (NA and 2,3-NA) with an overall 83% (5 out of 6) success rate, as confirmed by subsequent experiments. As ΔE only requires simple ground-state calculations on monomer candidates, it can be easily implemented and scalable for wide-range material screening or even used as a data training set for machine learning protocol. We expect that the refinement of the ΔE threshold can expedite the further development of heavy-atom free organic materials with bright and persistent RTP. Currently, we are expanding the usage of ΔE for screening guest emitters from commercially available molecules to build a library of host-guest RTP mixtures.

Acknowledgements

The authors thank the support from A*STAR under its Advanced Manufacturing and Engineering Program (A2083c0051), the Ministry of Education, Singapore (MOE-MOET2EP10120-0007), the Singapore University of Technology and Design [SUTD-ZJU (VP) 201905], the National Natural Science Foundation of China (21820102005, 22072084, 22078314, 21878286, 21908216), and Dalian Institute of Chemical Physics (DICPI201938, DICPZZBS201805). The authors are grateful for the supercomputing resources of SUTD-MIT IDC and the National Supercomputing Centre (Singapore). This graphical abstract has been designed using resources from flaticon.com with authors: Good Ware, Freepik.com, and Cursor Creative.

Conflict of Interest

The authors declare no conflict of interest.

Data Availability Statement

The data that support the findings of this study are available in the supplementary material of this article.

Keywords: Afterglow Emission · Charge-Transfer State · Excited States · Intersystem Crossing · Room-Temperature Phosphorescence

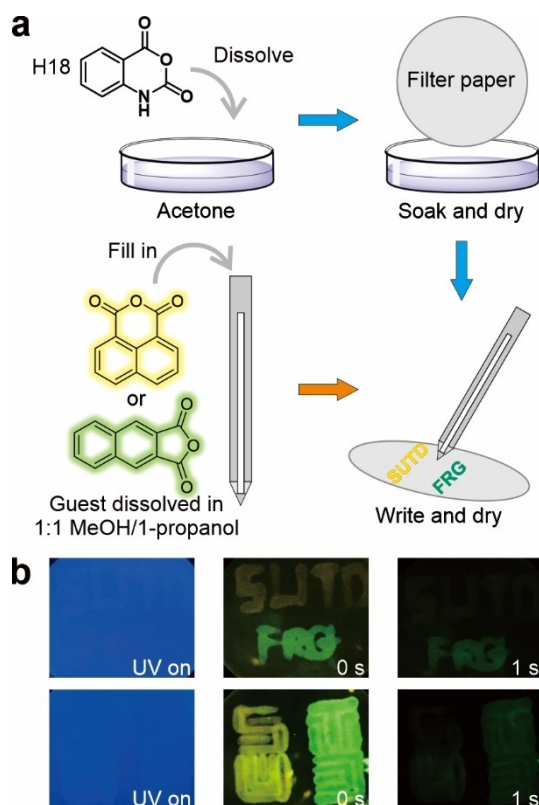


Figure 4. a) Application procedure on applying RTP combos for message encryption. b) Multi-layer encryption using H18 with NA (yellow afterglow with shorter lifetime) as the first-layer message and 2,3-NA (green afterglow with longer lifetime) as the second-layer message, using a paintbrush for applying guest (top) and using masking and a paintbrush for applying guest (bottom) with excitation light at 254 nm.

- [1] R. Kabe, C. Adachi, *Nature* **2017**, *550*, 384–387.
- [2] W. Zhao, Z. He, B. Z. Tang, *Nat. Rev. Mater.* **2020**, *5*, 869–885.
- [3] R. Kabe, N. Notsuka, K. Yoshida, C. Adachi, *Adv. Mater.* **2016**, *28*, 655–660.
- [4] L. Bian, H. Shi, X. Wang, K. Ling, H. Ma, M. Li, Z. Cheng, C. Ma, S. Cai, Q. Wu, N. Gan, X. Xu, Z. An, W. Huang, *J. Am. Chem. Soc.* **2018**, *140*, 10734–10739.
- [5] X. Ma, C. Xu, J. Wang, H. Tian, *Angew. Chem. Int. Ed.* **2018**, *57*, 10854–10858; *Angew. Chem.* **2018**, *130*, 11020–11024.
- [6] Z. An, C. Zheng, Y. Tao, R. Chen, H. Shi, T. Chen, Z. Wang, H. Li, R. Deng, X. Liu, W. Huang, *Nat. Mater.* **2015**, *14*, 685–690.
- [7] Y. Deng, D. Zhao, X. Chen, F. Wang, H. Song, D. Shen, *Chem. Commun.* **2013**, *49*, 5751–5753.
- [8] Q. Feng, Z. Xie, M. Zheng, *Chem. Eng. J.* **2021**, *420*, 127647.
- [9] P. She, Y. Qin, Y. Ma, F. Li, J. Lu, P. Dai, H. Hu, X. Liu, S. Liu, W. Huang, Q. Zhao, *Sci. China Mater.* **2021**, *64*, 1485–1494.
- [10] J. Yang, X. Zhen, B. Wang, X. Gao, Z. Ren, J. Wang, Y. Xie, J. Li, Q. Peng, K. Pu, Z. Li, *Nat. Commun.* **2018**, *9*, 840.
- [11] X. Zhen, Y. Tao, Z. An, P. Chen, C. Xu, R. Chen, W. Huang, K. Pu, *Adv. Mater.* **2017**, *29*, 1606665.
- [12] Kenry, C. Chen, B. Liu, *Nat. Commun.* **2019**, *10*, 2111.
- [13] W. Zhao, Z. He, Jacky W. Y. Lam, Q. Peng, H. Ma, Z. Shuai, G. Bai, J. Hao, Ben Z. Tang, *Chem* **2016**, *1*, 592–602.
- [14] W. Huang, B. Chen, G. Zhang, *Chem. Eur. J.* **2019**, *25*, 12497–12501.
- [15] Z.-Y. Zhang, Y. Chen, Y. Liu, *Angew. Chem. Int. Ed.* **2019**, *58*, 6028–6032; *Angew. Chem.* **2019**, *131*, 6089–6093.
- [16] M.-M. Fang, J. Yang, Z. Li, *Chin. J. Polym. Sci.* **2019**, *37*, 383–393.
- [17] S. Cai, H. Ma, H. Shi, H. Wang, X. Wang, L. Xiao, W. Ye, K. Huang, X. Cao, N. Gan, C. Ma, M. Gu, L. Song, H. Xu, Y. Tao, C. Zhang, W. Yao, Z. An, W. Huang, *Nat. Commun.* **2019**, *10*, 4247.
- [18] J. Yang, Z. Ren, B. Chen, M. Fang, Z. Zhao, B. Z. Tang, Q. Peng, Z. Li, *J. Mater. Chem. C* **2017**, *5*, 9242–9246.
- [19] C. Zhao, Y. Jin, J. Wang, X. Cao, X. Ma, H. Tian, *Chem. Commun.* **2019**, *55*, 5355–5358.
- [20] X. Ma, J. Wang, H. Tian, *Acc. Chem. Res.* **2019**, *52*, 738–748.
- [21] X. Zhang, L. Du, W. Zhao, Z. Zhao, Y. Xiong, X. He, P. F. Gao, P. Alam, C. Wang, Z. Li, J. Leng, J. Liu, C. Zhou, J. W. Y. Lam, D. L. Phillips, G. Zhang, B. Z. Tang, *Nat. Commun.* **2019**, *10*, 5161.
- [22] F. Clabau, X. Rocquefelte, S. Jobic, P. Deniard, M. H. Whangbo, A. Garcia, T. Le Mercier, *Chem. Mater.* **2005**, *17*, 3904–3912.
- [23] C. Chen, Z. Chi, K. C. Chong, A. S. Batsanov, Z. Yang, Z. Mao, Z. Yang, B. Liu, *Nat. Mater.* **2021**, *20*, 175–180.
- [24] B. Ding, L. Ma, Z. Huang, X. Ma, H. Tian, *Sci. Adv.* **2021**, *7*, eabf9668.
- [25] H. Ma, Q. Peng, Z. An, W. Huang, Z. Shuai, *J. Am. Chem. Soc.* **2019**, *141*, 1010–1015.
- [26] Y. Dong, A. A. Sukhanov, J. Zhao, A. Elmali, X. Li, B. Dick, A. Karatay, V. K. Voronkova, *J. Phys. Chem. C* **2019**, *123*, 22793–22811.
- [27] Y. Mu, Z. Yang, J. Chen, Z. Yang, W. Li, X. Tan, Z. Mao, T. Yu, J. Zhao, S. Zheng, S. Liu, Y. Zhang, Z. Chi, J. Xu, M. P. Aldred, *Chem. Sci.* **2018**, *9*, 3782–3787.
- [28] Z. Yang, Z. Mao, X. Zhang, D. Ou, M. Yingxiao, Y. Zhang, C. Zhao, S. Liu, Z. Chi, J. Xu, Y.-C. Wu, P.-Y. Lu, A. Lien, M. Bryce, *Angew. Chem. Int. Ed.* **2016**, *55*, 2181–2185; *Angew. Chem.* **2016**, *128*, 2221–2225.
- [29] Y. Xiong, Z. Zhao, W. Zhao, H. Ma, Q. Peng, Z. He, X. Zhang, Y. Chen, X. He, J. W. Y. Lam, B. Z. Tang, *Angew. Chem. Int. Ed.* **2018**, *57*, 7997–8001; *Angew. Chem.* **2018**, *130*, 8129–8133.
- [30] X. Chen, C. Xu, T. Wang, C. Zhou, J. Du, Z. Wang, H. Xu, T. Xie, G. Bi, J. Jiang, X. Zhang, J. N. Demas, C. O. Trindle, Y. Luo, G. Zhang, *Angew. Chem. Int. Ed.* **2016**, *55*, 9872–9876; *Angew. Chem.* **2016**, *128*, 10026–10030.
- [31] M. Li, K. Ling, H. Shi, N. Gan, L. Song, S. Cai, Z. Cheng, L. Gu, X. Wang, C. Ma, M. Gu, Q. Wu, L. Bian, M. Liu, Z. An, H. Ma, W. Huang, *Adv. Opt. Mater.* **2019**, *7*, 1800820.
- [32] Y. Wang, J. Yang, M. Fang, Y. Yu, B. Zou, L. Wang, Y. Tian, J. Cheng, B. Z. Tang, Z. Li, *Matter* **2020**, *3*, 449–463.
- [33] R. L. Martin, *J. Chem. Phys.* **2003**, *118*, 4775–4777.
- [34] C. A. Guido, P. Cortona, B. Mennucci, C. Adamo, *J. Chem. Theory Comput.* **2013**, *9*, 3118–3126.
- [35] G. Baryshnikov, B. Minaev, H. Ågren, *Chem. Rev.* **2017**, *117*, 6500–6537.
- [36] C. M. Marian, *Wiley Interdiscip. Rev.: Comput. Mol. Sci.* **2012**, *2*, 187–203.
- [37] B. F. Habenicht, O. V. Prezhdo, *J. Am. Chem. Soc.* **2012**, *134*, 15648–15651.
- [38] S. K. Lower, M. A. El-Sayed, *Chem. Rev.* **1966**, *66*, 199–241.
- [39] S. Hirata, *J. Phys. Chem. Lett.* **2018**, *9*, 4251–4259.
- [40] B. Chen, W. Huang, X. Nie, F. Liao, H. Miao, X. Zhang, G. Zhang, *Angew. Chem. Int. Ed.* **2021**, *60*, 16970–16973; *Angew. Chem.* **2021**, *133*, 17107–17110.
- [41] Y. Lei, J. Yang, W. Dai, Y. Lan, J. Yang, X. Zheng, J. Shi, B. Tong, Z. Cai, Y. Dong, *Chem. Sci.* **2021**, *12*, 6518–6525.
- [42] W. Chi, J. Chen, W. Liu, C. Wang, Q. Qi, Q. Qiao, T. M. Tan, K. Xiong, X. Liu, K. Kang, Y.-T. Chang, Z. Xu, X. Liu, *J. Am. Chem. Soc.* **2020**, *142*, 6777–6785.
- [43] X. Zhao, Q. Yao, S. Long, W. Chi, Y. Yang, D. Tan, X. Liu, H. Huang, W. Sun, J. Du, J. Fan, X. Peng, *J. Am. Chem. Soc.* **2021**, *143*, 12345–12354.

Manuscript received: January 11, 2022

Accepted manuscript online: February 2, 2022

Version of record online: February 15, 2022